Folding of ω-Conotoxins. 1. Efficient Disulfide-Coupled Folding of Mature Sequences in Vitro†

Marian Price-Carter, William R. Gray, and David P. Goldenberg*

Department of Biology, University of Utah, Salt Lake City, Utah 84112

Received June 28, 1996; Revised Manuscript Received September 18, 1996⊗

ABSTRACT: Disulfide-coupled refolding reactions of five ω-conotoxins, Ca^{2+} channel antagonists derived from marine snails of the genus *Conus*, were examined. These peptides are 23−26 amino acid residues long, and the native conformation of each is stabilized by three disulfide bonds. Although the primary structures of the peptides show only limited sequence similarity, the patterns of disulfides and three-dimensional conformations are very similar. Refolding of the reduced proteins was promoted by the disulfide form of glutathione (GSSG) in the presence of reduced glutathione (GSH). All five of the peptides examined were able to refold to the native conformation, as judged by reversed-phase HPLC behavior, with efficiencies of 16% for ω-MVIIC, 28% for ω-MVIID, and 50% for ω-MVIIA, ω-GVIA, and ω-SVIA. The refolded form of ω-MVIIA was further shown to have biological activity indistinguishable from that of the native form, as well as the same rate of reductive unfolding in the presence of dithiothreitol. The overall folding rate and efficiency of ω-MVIIA was found to be quite sensitive to the thiol−disulfide redox potential, with optimum rates and yields obtained in the presence of GSSG and GSH at concentrations similar to those believed to be present in the endoplasmic reticulum. The folding efficiency of this peptide was greatly reduced by the addition of 8 M urea, indicating that formation of the correct disulfides is determined largely by noncovalent interactions, as opposed to steric constraints arising from the spacing between Cys residues. These results demonstrate that the mature forms of at least some ω-conotoxins contain sufficient information to direct correct folding and disulfide formation, in spite of their small size and limited sequence conservation.

Marine snails of the genus *Conus* produce remarkably potent paralytic venoms that enable the snails to prey on a variety of other marine animals, including mollusks, worms, and fish (Gray et al., 1988; Olivera et al., 1990, 1991). The *Conus* venoms have been characterized extensively and have been found to contain large numbers of peptides ranging in size from approximately 12 to 30 amino acid residues. Peptides isolated from the venoms bind tightly and specifically to a variety of ion channels and receptors of the neuromusculature, and they have become valuable reagents for studying the molecular components of the nervous system. The peptides with known activities are referred to collectively as conotoxins and are classified according to their molecular targets (Gray et al., 1988).

In spite of their small size, many of the conotoxins fold into well-defined three-dimensional conformations, several of which have been determined by high-resolution NMR spectroscopy (Kobayashi et al., 1989; Pardi et al., 1989; Davis et al., 1993; Pallaghy et al., 1993; Skalicky et al., 1993; Sevilla et al., 1993; Basus et al., 1995; Farr-Jones et al., 1995; Kohno et al., 1995). The NMR-derived structure of one such peptide, toxin ω-MVIIA (Basus et al., 1995; Kohno et al., 1995), isolated from the venom of *Conus magus*, is illustrated in Figure 1a. This toxin is a member of the ω-class of peptides, which are characterized by their ability to bind to and inhibit presynaptic Ca^{2+} channels (Olivera et al., 1994). Like most of the *Conus* peptides, the ω-toxins contain a high density of disulfide bonds, in this case 3 disulfides in a peptide of only 25 residues. Other members of the ω-class

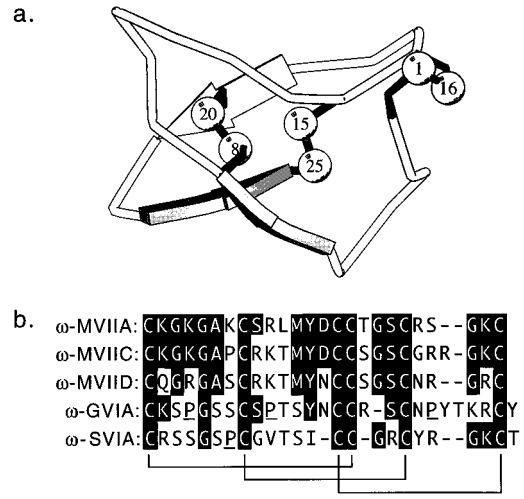

FIGURE 1: Three-dimensional structure of ω-conotoxin MVIIA and primary structures of related conotoxins. (a) Ribbon diagram of the three-dimensional structure of ω-MVIIA, drawn from an NMR solution structure determined by Kohno et al. (1995). The disulfide-linked Cys sulfur atoms are shown as circles labeled with the residue numbers. The figure was drawn using the MOLSCRIPT program of Per Kraulis. (b) Aligned sequences of the ω-conotoxins used in this study. Shaded regions indicate portions of the sequences that are identical to the corresponding residues of ω-MVIIA. The disulfide linkages that have been either determined directly (Chung et al., 1995) or inferred are represented by the solid lines below the ω-SVIA sequence. Hydroxylated Pro residues are indicated by underscores. All of the peptides have amidated carboxyl termini. The sources of the sequences are listed under Experimental Procedures.

† Supported by NSF Grant MCB-9316065 and NIH Grant GM42494.
* Corresponding author.
⊗ Abstract published in *Advance ACS Abstracts,* November 15, 1996.

S0006-2960(96)01574-7 CCC: $12.00 © 1996 American Chemical Society

display the same pattern of Cys spacings and, where known, the same disulfide pairings and similar three-dimensional conformations. Sequences of some of the other members of this class of peptides are shown in Figure 1b. Apart from the Cys residues, there is very little sequence identity among the ω-toxins isolated from different species, although all of the sequences are characterized by a preponderance of polar residues. Interestingly, the same overall fold and pattern of disulfide bonds has been found in other, apparently unrelated, peptides (Pallaghy et al., 1994). It thus appears that this small structural motif is capable of accommodating a wide variety of sequences and biological functions.

Although the disulfide bonds in the conotoxins are known to be important in maintaining their biologically active three-dimensional structures, how these disulfides are able to form specifically has been unclear. Analyses of cDNA sequences encoding conotoxins have revealed that, like other secreted disulfide-bonded proteins, the peptides are made as precursors containing signal sequences for targeting to the endoplasmic reticulum (Woodward et al., 1990; Colledge et al., 1992; Olivera et al., 1990, 1991). The peptides are believed to undergo disulfide-coupled folding in the lumen of the endoplasmic reticulum in the presence of both oxidized and reduced glutathione (GSSG and GSH,[1] respectively) and the enzyme protein disulfide isomerase. Under these conditions, disulfide formation is expected to be freely reversible, allowing the possible disulfide-bonded isomers to accumulate according to their relative stabilities. Studies of other disulfide-containing proteins, including bovine pancreatic trypsin inhibitor (BPTI) (Creighton, 1990, 1992; Weissman & Kim, 1991; Goldenberg, 1992), ribonuclease A (Wearne & Creighton, 1988; Rothwarf & Scheraga, 1993; Li et al., 1995), and ribonuclease T1 (Pace & Creighton, 1986) have demonstrated that folding and disulfide bond formation are thermodynamically coupled processes and that the specificity of disulfide formation is determined by the extent to which noncovalent interactions favor conformations in which the Cys thiols are positioned to interact. The conotoxins, however, are much smaller than these proteins and display a high degree of sequence variability, even among functionally and structurally related toxins. It is, therefore, possible that the mature sequences do not contain sufficient information to specify correct disulfide formation and folding.

The cDNA sequences also predict that the precursor forms of *Conus* toxins contain a propeptide located between the signal sequence and the sequence of the mature peptide (Woodward et al., 1990; Colledge et al., 1992; Olivera et al., 1990, 1991). Within a class of toxins, such as the ω-toxins, the propeptide sequences are much more highly conserved than the mature sequences. Different classes of toxins, however, have different propeptides, along with different three-dimensional conformations and patterns of disulfide bonds. These observations have led Olivera et al. (1990, 1991) to propose that the propeptides may play an active role in directing folding and disulfide formation.

We have begun investigating what factors are important for enabling *Conus* peptides to fold by examining the folding of mature ω-conotoxins under conditions similar to those found in the endoplasmic reticulum. The experiments described here indicate that the reduced forms of five different mature toxins, derived from three *Conus* species, are able to refold correctly in the presence of oxidized and reduced glutathione, with efficiencies ranging from 15% to 50%. The distributions of disulfide-bonded species observed under different conditions indicate that the mature sequences do, in fact, contain information specifying the correct conformation but that the stability of this conformation, relative to other possible forms, is marginal. In the accompanying paper, we describe folding experiments with precursor forms of one of the toxins, ω-MVIIA, in the presence and absence of protein disulfide isomerase.

EXPERIMENTAL PROCEDURES

Conus Toxins. All of the toxins used in these studies were chemically synthesized on the basis of previously determined sequences of the natural toxins [ω-GVIA (Olivera et al., 1984), ω-MVIIA (Olivera et al., 1987), and ω-SVIA (Ramilo et al., 1992)] or cDNA clones [ω-MVIIC (Hillyard et al., 1992) and ω-MVIID (Monje et al., 1993)]. Samples of synthetic ω-MVIIA were generous gifts of Drs. George Miljanich (Neurex Corp.) and Michael Gerlander (Bachem Inc., Torrance, CA). The two samples used in these studies displayed indistinguishable folding properties. Conotoxins ω-GVIA and ω-SVIA were kindly provided by Dr. B. M. Olivera. The synthetic versions of ω-GVIA, ω-MVIIA, and ω-SVIA contained the modified residues found in the natural peptides, specifically amidated C-terminal residues, and, in the cases of ω-GVIA and ω-SVIA, hydroxylated prolines. For the peptides derived from cDNA sequences, the C-terminal residues were amidated, but the prolyl residues were not hydroxylated. The starting forms of the peptides contained the three native disulfides indicated in Figure 1b (Chung et al., 1995).

Relative concentrations of different forms of ω-MVIIA were routinely determined from the peak areas of reversed-phase HPLC profiles. Relative concentrations were converted to absolute concentrations using the measured peak area for a sample of native ω-MVIIA for which the concentration had been determined from the absorbance at 274.5 nm, assuming an extinction coefficient of 1400 M^{-1} cm^{-1} for the single Tyr residue of the peptide (Glazer, 1976). Concentrations of other peptides were determined from amino acid analyses.

Reversed-Phase High-Performance Liquid Chromatography. Various disulfide-bonded or reduced forms of the toxins were separated by reversed-phase HPLC using a Vydac C_{18} column (4.6 mm inside diameter × 25 cm long) eluted with a gradient of acetonitrile (CH_3CN) in trifluoroacetic acid (TFA) at a flow rate of 1 mL/min. Gradients were prepared by mixing two buffer solutions: A (0.103% TFA) and B (0.96% TFA and 60% CH_3CN). Refolding and unfolding mixtures involving either ω-MVIIA or ω-GVIA were fractionated using a linear gradient of 15−32% buffer B. For ω-MVIIC, a linear gradient of 10−27% buffer B was used, and a 10−30% gradient was used for both ω-MVIID and ω-SVIA. In all separations, the concentration of buffer B was increased at a rate of 0.5%/min. Elution profiles were

[1] Abbreviations: GSSG and GSH, disulfide and thiol forms, respectively, of glutathione; DTT, dithiothreitol; Tris-HCl, tris(hydroxymethyl)aminomethane hydrochloride; MOPS, 3-(*N*-morpholino)-propanesulfonic acid; Hepes, *N*-(2-hydroxyethyl)piperazine-*N*′-2-ethanesulfonic acid; EDTA, ethylenediaminetetraacetic acid; TFA, trifluoroacetic acid; HPLC, high-performance liquid chromatography; RNase A, ribonuclease A; BPTI, bovine pancreatic trypsin inhibitor.

monitored by absorbance at 220 nm. Absorption data were collected and analyzed using the Rainin Dynamax computer interface and software. Relative concentrations of the various species were calculated by integrating the appropriate HPLC peaks.

Preparation of Reduced Toxins. To prepare fully reduced toxins for folding experiments, 20−80 μM peptide was incubated with 50 mM dithiothreitol (DTT) in the presence of 0.1 M Tris-HCl, pH 8.7, 0.2 M KCl, and 0.001 M EDTA under a N_2 atmosphere. After 45 min at room temperature, the pH of the solution was lowered to about 2 by the addition of 0.05 volume of concentrated phosphoric acid. The reduced peptide was then separated from the DTT and other buffer components by reversed-phase HPLC. The reduced peptides were lyophilized and stored at −20 °C.

Reduced and carboxamidomethylated peptides were prepared by incubating the peptides with DTT under the conditions described above for 45 min and then adding an equal volume of 0.5 M iodoacetamide and 0.5 M Tris-HCl, pH 6.8. After incubation for an additional 2 min at room temperature, the peptide was separated from the other reagents by HPLC.

Disulfide-Coupled Folding and Unfolding Reactions. For folding experiments, reduced and lyophilized peptide was dissolved in 10 mM HCl to a final concentration of 40 μM. The dissolved peptide was then mixed with an equal volume of 0.2 M MOPS, pH 7.3, 0.4 M KCl, 2 mM EDTA, and mixtures of GSSG and GSH as appropriate for the particular experiment. In a typical experiment, a total of 20 nmol of peptide was used in a reaction volume of 1 mL, and 100−200-μL samples were withdrawn, quenched, and analyzed.

Folding experiments in the presence of 8 M urea were carried out as described above, except that the peptide was dissolved in 10 mM HCl to a concentration of 160 μM and then mixed with 7 volumes of a solution containing 9.14 M urea, 0.114 M MOPS, pH 7.3, 0.229 M KCl, 1.14 mM EDTA, and appropriate concentrations of GSSG and GSH.

Reductive unfolding experiments in the presence of GSH were carried out as described above, except that the reactions were initiated with native peptide. Reduction reactions in the presence of DTT were carried out in the presence of 0.1 M Tris-HCl, pH 8.7, 0.2 M KCl, and 0.001 M EDTA.

At various times after initiation of either folding or unfolding reactions, aliquots were removed and quenched by mixing with 0.05 volume of concentrated phosphoric acid. The trapped species were then separated by reversed-phase HPLC.

All solutions used for folding and unfolding experiments were flushed with N_2 and the reactions were carried out in septum vials under an N_2 atmosphere.

The kinetics of folding and unfolding were analyzed by comparing the observed time-dependent changes in concentration of the native protein with those predicted by numerical simulations. The simulations were performed using the program HopKINSIM, a version of KINSIM (Frieden, 1993) adapted for the Apple Macintosh.

Ca^{2+} Channel Binding Assay. The biological activities of different forms of ω-MVIIA were determined by measuring binding to Ca^{2+} channels present in crude preparations of chick brain presynaptic membranes (synaptosomes) (Cruz & Olivera, 1986; Olivera et al., 1987). Binding was detected as the blocking of sites otherwise available for binding to radiolabeled ω-GVIA.

To generate a binding curve, various amounts of peptide were mixed with a fixed quantity of synaptosomes (containing approximately 30 μg of total protein and 200 fmol of ω-toxin binding sites) to yield 45-μL reaction mixtures also containing 0.32 M sucrose, 5 mM Hepes−Tris, pH 7.4, 2 mg/mL hen egg white lysozyme, and 0.1 M NaCl. The mixtures were incubated in siliconized γ-counting tubes for 30 min on ice. After this incubation, 5 μL of a solution containing 500−1000 fmol of ^{125}I-labeled ω-GVIA was added to each tube and the solutions were allowed to incubate for another 30 min at room temperature. During this incubation, the total γ-radioactivity in each tube (typically 50 000 counts/min) was determined using a Packard Multi-Prias-1 counter. The solution was then diluted with 3 mL of ice-cold wash buffer containing 10 mM Hepes−Tris, pH 7.4, 0.1 M choline chloride, 0.1% bovine serum albumin, and 0.05% Tween 20. The radiolabeled ω-GVIA bound to the membrane receptors was then separated from unbound label by filtration through Whatman GF/C glass fiber filters that had previously been soaked in 0.2% poly(ethylenimine). The tubes were rinsed twice with 3-mL aliquots of wash buffer, and the rinse solutions were passed through the same glass fiber disks. The radioactivity captured on each filter was then determined. For each sample, the radioactivity bound to the synaptosome membranes was normalized by dividing by the total radioactivity measured in the incubation tube before filtration of the sample.

The number of sites occupied by unlabeled peptide was taken to be proportional to the difference between the normalized radioactivity bound in the absence of added ω-MVIIA and that bound in the presence of the unlabeled sample. The total number of receptor sites available for ω-MVIIA binding was assumed to be proportional to the radioactivity bound in the absence of ω-MVIIA minus that bound after incubation with saturating concentrations of native ω-MVIIA. Typically, 20−30% of the sites were occupied by radiolabeled ω-GVIA in the presence of the highest concentrations of ω-MVIIA, presumably reflecting nonspecific binding of the labeled peptide and, possibly, the presence of receptor subclasses to which only ω-GVIA binds.

The fraction of sites occupied, f_{occ}, in the presence of a given concentration of ω-MVIIA was determined as

$$f_{occ} = \frac{\text{sites occupied}}{\text{total sites}} = \frac{^{125}\text{I bound (w/o } \omega\text{-MVIIA)} - ^{125}\text{I bound (w/sample)}}{^{125}\text{I bound (w/o } \omega\text{-MVIIA)} - ^{125}\text{I bound (w/saturating } \omega\text{-MVIIA)}} \quad (1)$$

The values determined from duplicate measurements were averaged and plotted as a function of total peptide concentration.

Calculations of Accessible Surface Area. The burial of individual atoms in the folded conformation of ω-MVIIA were calculated using the algorithm of Lee and Richards (1971), as implemented in the program ACCESS by T. J. Richmond, and the group radii of Chothia (1975). The coordinates for 13 energy-minimized NMR structures of folded ω-MVIIA were kindly provided by Dr. T. Kohno (entry 1OMG in the Brookhaven Protein Data Bank), and solvent accessibilities were calculated for each of these structures and the results averaged. To approximate the accessibility of each residue in the unfolded polypeptide,

accessibilities were calculated for Cys-Gly, Gly-X-Gly, and Gly-Cys-NH_2 peptides, corresponding to the N-terminal, internal, and C-terminal residues of ω-MVIIA, respectively. The peptide model for each residue was constructed with an extended backbone conformation ($\phi = -120°$, $\psi = 140°$) and side-chain dihedral angles corresponding to the predominant rotamer conformation identified by Ponder and Richards (1987). Buried surface area was defined as the difference between the accessible surface area for an atom or group in the extended conformation and that in the folded conformation. All nitrogen and oxygen atoms were classified as polar, while carbon and sulfur atoms were classified as nonpolar.

RESULTS

The peptide used for most of the experiments described here was ω-MVIIA, originally isolated from the venom of *Conus magus* (Olivera et al., 1987). This peptide was chosen because, in contrast to many other *Conus* toxins, the mature form does not contain any posttranslationally modified amino acid residues other than an amidated C-terminal Cys. Thus, analogs of the precursor forms can be synthesized in bacteria and their folding can be compared with that of the mature sequence, as described in the accompanying paper, without the complications that might arise from other modifications.

Disulfide-Coupled Folding of ω-MVIIA. The cDNA sequences determined by Hillyard, Olivera, and their colleagues (Woodward et al., 1990; Colledge et al., 1992) indicate that the *Conus* toxins are synthesized as precursors containing a leader peptide to direct the polypeptides to the endoplasmic reticulum, where they presumably fold and form their disulfides. The secretory organelles of eukaryotic cells have been shown to contain relatively high concentrations of both oxidized and reduced glutathione, which are believed to participate either directly or indirectly in the formation and rearrangement of disulfide bonds in newly synthesized polypeptides (Hwang et al, 1992). We thus began our characterization of the folding of *Conus* toxins by following the disulfide-coupled folding of reduced ω-MVIIA in the presence of GSSG and GSH at concentrations similar to those found in the secretory organelles, i.e., 0.25−1 mM GSSG and 0−8 mM GSH.

Figure 2 shows HPLC profiles of the disulfide-bonded forms of ω-MVIIA trapped after various times of refolding in the presence of 1 mM GSSG, with and without added GSH. Under the chromatographic conditions used here, molecules with the largest fraction of exposed nonpolar surface area are expected to elute last from the C_{18} column. In accordance with this expectation, the fully reduced peptide eluted much later than the native peptide and later than any of the other species that accumulated during folding.

The distribution of species generated during the folding in the presence of 1 mM GSSG and no GSH is illustrated in the leftmost set of HPLC traces in Figure 2. Within 15 min, the distribution was dominated by three major HPLC peaks, along with two smaller peaks. One of the smaller peaks had the HPLC retention time of the native peptide (labeled N), while of the other four species (labeled with asterisks), three had shorter retention times and the fourth eluted after the native form. Between 15 and 90 min after initiation of folding, there was very little change in the distribution, but at later times the four nonnative species were slowly converted to molecules with the retention time of the native peptide.

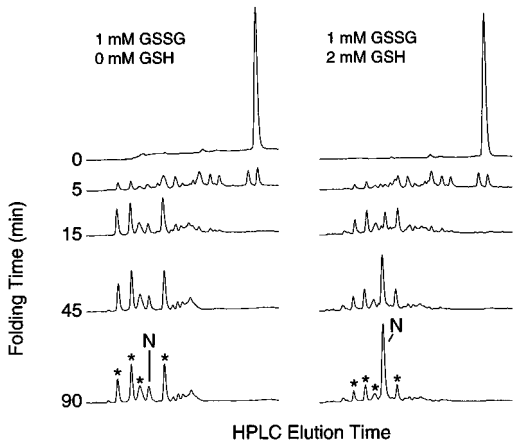

FIGURE 2: Refolding of reduced ω-MVIIA in the presence of oxidized and reduced glutathione. Reduced peptide was refolded in the presence of 1 mM GSSG and either 0 or 2 mM GSH, as indicated, at 25 °C in a buffer containing 0.1 M MOPS, pH 7.3, 0.2 M KCl, and 1 mM EDTA. At the indicated times, samples of the reaction mixtures were withdrawn, mixed with 0.05 volume of H_3PO_4, and fractionated by reversed-phase HPLC, as described under Experimental Procedures. The traces represent absorbance at 220 nm monitored from approximately 30 to 55 min after injection. N indicates the peak with the elution time of the native peptide and the asterisks identify the four peaks, discussed in the text, that appear early in folding and are converted to the native form in a process facilitated by GSH.

When refolding was carried out in the presence of 1 mM GSSG and 2 mM GSH, the initial distribution of disulfide-bonded species was similar to that seen in the absence of GSH. At later times, however, the appearance of molecules with the retention time of the native protein was much faster in the presence of the thiol reagent. After 90 min of folding, the material in the peak labeled N represented approximately 50% of the total protein, and there was little or no change in this distribution at later times. Although it is possible that the peak labeled N contained species other than the correctly refolded form, this material was found to display the same biological activity as the starting sample (see below). The same HPLC profile was generated by incubating the native protein with 1 mM GSSG and 2 mM GSH, indicating that the final yield of native protein under these conditions represents an equilibrium distribution among the various disulfide-bonded species. In the presence of higher concentrations of GSH (4 and 8 mM), the yield of native peptide decreased substantially, with a concomitant increase in the final levels of molecules with retention times intermediate between those of the native and fully reduced forms, as well as some molecules that eluted before the native peptide. These species are most likely intermediates containing one or two disulfide bonds.

As described above, the four peaks labeled with asterisks in Figure 2 appeared quite early in folding and were then converted to the native form via a process that was facilitated by GSH. This behavior suggested that these species might contain either nonnative disulfides or mixed disulfides with glutathione that must be reduced in order to allow conversion to the native form. In order to characterize these molecules, the reduced protein was refolded for 4 h in the presence of 1 mM GSSG without GSH, and the material in the four peaks described above, along with that in the peak with the native

retention time, was collected and subjected to electrospray ionization mass spectroscopy. The major components in each of these peaks were found to have molecular masses within 1 Da of that expected for ω-MVIIA with three disulfide bonds (2639.1), demonstrating that none of them contained mixed disulfides. In addition, the relative final yields of all five species appeared to be constant in the presence of different concentrations of GSSG and GSH, indicating that they all contained the same number of intramolecular disulfides, most likely three.

To analyze the folding behavior more quantitatively, the observed kinetics of appearance of the native form were compared with predictions of the following simple model:

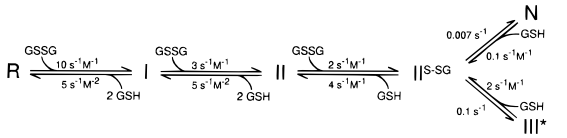

(2)

In this model, R, I, and II represent populations of molecules with zero, one, or two intramolecular disulfides, respectively, while II^{S-SG} represents a population of molecules, each containing two intramolecular disulfides and a glutathione mixed disulfide, which can form a third disulfide to yield either the native peptide (N) or the various nonnative forms, indicated as III* in the scheme. For simplicity, the requisite mixed-disulfide intermediates in the formation of the first and second disulfides are not treated explicitly. Instead, the rates of disulfide formation are assumed to be determined by the rate of forming the mixed disulfide in a second-order reaction with GSSG, as expected for a typical peptide disulfide-formation reaction in the presence of mM GSSG concentrations, and the rates of reduction of molecules in populations I and II are assumed to be second-order with respect to GSH.

The rate constants in the scheme were adjusted to obtain a good fit between the observed and predicted folding kinetics in the presence of various concentrations of GSSG and GSH, as well as consistency with the equilibration and reductive unfolding experiments described below. These rate constants lie within the range observed for disulfide formation and reduction reactions in model compounds and other proteins under similar conditions (Szajewski & Whitesides, 1980; Creighton & Goldenberg, 1984; Snyder, 1987; Zhang & Snyder, 1989, 1991; Rothwarf & Scheraga, 1992). Most of the observed folding kinetics could also be predicted by a slightly simpler model in which the mixed disulfide intermediates in the formation of N and III* are not treated explicitly, as in the earlier steps in the scheme above. This model, however, required unrealistically high values for the rate constants for forming N and III* directly from II and was not able to predict the observed rates of reduction of N in the presence of GSH.

In Figure 3, the observed time courses for appearance of the native peptide in the presence of 1 mM GSSG and 0, 2, 4, and 8 mM GSH are compared with those predicted by the model. As shown, the model predicts accurately the overall folding rate, the biphasic kinetics for forming the native form in the absence of GSH, and the decreased final yield of N in the presence of increasing GSH concentrations. Consistency between observed and predicted folding kinetics was also found for experiments with lower concentrations of GSSG (0.25 and 0.5 mM), where lower overall rates were observed.

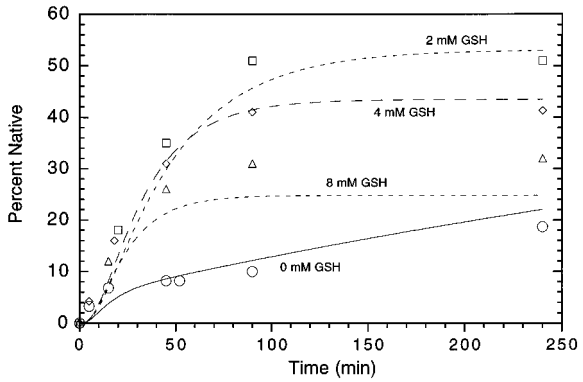

FIGURE 3: Folding kinetics of ω-MVIIA in the presence of GSSG and GSH. Fully reduced peptide was refolded in the presence of 1 mM GSSG and 2 mM (□), 4 mM (◇), 8 mM (△), or no (○) GSH. The disulfide-bonded species present at the indicated times were fractionated by HPLC, and the fraction of native peptide was determined from the relative area of the peak labeled N in Figure 2. The curves in the figure were generated by numerical integration of the rate expressions corresponding to the kinetic scheme and rate constants shown in eq 2.

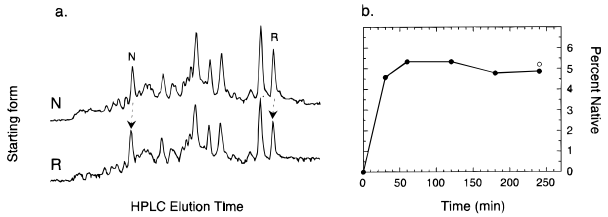

FIGURE 4: Equilibration between the native and fully reduced forms of ω-conotoxin MVIIA. (a) Reversed-phase HPLC separations of disulfide-bonded species generated by equilibrating either native (upper trace) or fully reduced peptide (lower trace) for 3 h in the presence of 1 mM GSSG and 20 mM GSH at 25 °C, pH 7.3. After equilibration, samples of the reaction mixtures were quenched and fractionated as described in the legend to Figure 2. The peaks with elution times of the native (N) and reduced (R) peptide are labeled. (b) Concentration of native peptide, expressed as percent of total peptide, after various times of incubation of the reduced peptide (●) under the equilibration conditions described above. The open circle shows the percent of native peptide remaining after incubation of the native peptide under the same conditions for 4 h. The relative concentrations of native and reduced peptide were determined from the HPLC peak areas.

In the presence of 1 mM GSSG and 20 mM GSH, it was possible to establish an apparent equilibrium in which both the native and fully reduced forms were detectable, at concentrations representing approximately 4% and 6% of the total peptide, respectively (Figure 4). Very similar distributions were observed whether the starting protein was in the native or reduced form. From this result, an overall equilibrium constant for forming the three disulfides of the native form was estimated:

$$K_{eq} = \frac{[N][GSH]^6}{[R][GSSG]^3} \approx 0.04\ M^3 \qquad (3)$$

consistent with the rate constants in the scheme shown in eq 2. As discussed further below, this value is considerably greater than that expected for forming three disulfides in a disordered polypeptide but is less than observed for other globular proteins.

The modest preference for the correct disulfides in ω-MVIIA could arise either from stabilizing noncovalent

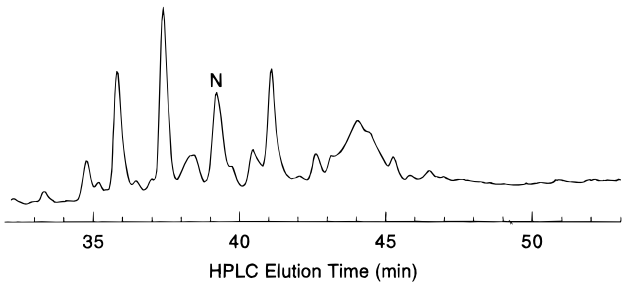

FIGURE 5: Refolding of reduced ω-MVIIA in the presence of 8 M urea. Fully reduced peptide was refolded in the presence of 8 M urea, 1 mM GSSG, and 2 mM GSH at 25 °C, pH 7.3, as described in the legend to Figure 2. At times ranging from 5 min to 26 h after the initiation of folding, samples of the reaction mixtures were withdrawn, mixed with 0.05 volume of H_3PO_4, and fractionated by reversed-phase HPLC. The HPLC trace shown in the figure represents the distribution at 360 min, at which time a final distribution appeared to have been established. The peak corresponding to the native form is labeled N.

interactions or from steric constraints in the small peptide. To determine whether the preference arises from steric constraints alone, disulfide-coupled folding was examined in the presence of a strong denaturant, 8 M urea. Figure 5 illustrates an HPLC profile representing the end point of a folding reaction containing 8 M urea, 1 mM GSSG, and 2 mM GSH. Comparison of this profile with those shown in Figure 2 indicates that the denaturant decreased significantly the yield of the native form, suggesting that noncovalent interactions are at least partially responsible for the relatively high yields of correctly folded peptide observed under optimal thiol−disulfide ratios. Interestingly, however, the distribution of disulfide-bonded forms observed at earlier times did not seem to be greatly affected by urea, suggesting that noncovalent interactions may not play a significant role in directing the initial stages of disulfide formation.

Biological Activity of Refolded ω-MVIIA. In order to determine whether the material in the major peak seen in the HPLC profiles of the refolding mixtures had the same conformation as the starting peptide with the three correct disulfides, its ability to bind to neuronal Ca^{2+} channels was measured (Cruz et al., 1986; Olivera et al., 1987). Samples of ω-MVIIA were mixed with chick brain synaptosomes, and after a 30-min equilibration period, an excess of ^{125}I-labeled ω-toxin GVIA was added and allowed to bind to any sites unoccupied by the ω-MVIIA. Unbound ^{125}I was removed by filtration and the amount of bound label was determined. Although the assay is not a rigorous measurement of the equilibrium dissociation constant, it displays a high degree of specificity and provides a qualitative measure of the affinity of the ω-toxins for their receptors. The affinities of different members of the ω-toxin family are readily distinguished by this assay (Hillyard et al., 1992; Ramilo et al., 1992; Monje et al., 1993), as are those of various modified forms (Kim et al., 1994, 1995; Nadasdi et al., 1995).

In Figure 6, the fraction of total sites blocked by ω-MVIIA at different concentrations is plotted as a function of total peptide concentration. Within the errors of the measurement, the refolded ω-MVIIA displayed the same binding behavior as the starting material. For both forms, the available sites were half-occupied at a ligand concentration of approximately 2×10^{-10} M, consistent with previous measurements of the affinity of this toxin for Ca^{2+} channels (Olivera et al., 1987; Hillyard et al., 1992; Kim et al., 1995). Fully reduced and alkylated ω-MVIIA was also assayed for its ability to bind to Ca^{2+} channels. As shown in Figure 6, there was no detectable binding of this form at concentrations up to 1 μM, indicating that either the reduction of the disulfides or the modification of the resulting thiols prevents stable binding to the receptor.

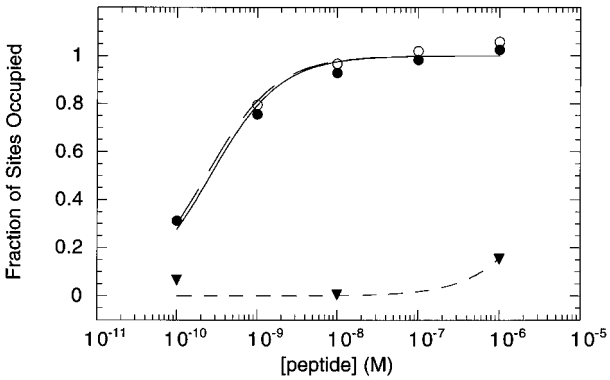

FIGURE 6: Receptor-binding activity of native and refolded ω-MVIIA. Samples of native (●) or refolded peptide (○) were incubated with chick brain synaptosomes, and the fraction of sites occupied was determined as the blocking of sites for subsequent binding by radiolabeled ω-GVIA, as described under Experimental Procedures. The much lower level of binding by ω-MVIIA that had been reduced and carboxamidomethylated is indicated by the filled triangles (▼). Each point represents the mean of two independent measurements. The curves represent nonlinear least-squares fits of the data to a simple binding isotherm, with apparent dissociation constants of 2.6×10^{-10} M, 2.3×10^{-10} M, and 5.4×10^{-6} M for the native, refolded, and reduced forms, respectively.

These results indicate that the refolded ω-MVIIA has biological activity that is indistinguishable from that of the starting native peptide. Together with the measurements of unfolding kinetics described below, these observations suggest that the refolded peptide found in the HPLC peak with the native elution time is, in fact, correctly refolded.

Reduction Kinetics of ω-MVIIA. The rate at which a protein disulfide bond is reduced by dithiothreitol (DTT) depends on the accessibility of the disulfide to the reagent and any strain that may destabilize the bond (Creighton, 1975, 1992; Singh & Whitesides, 1990; Goldenberg et al., 1993). Reduction kinetics can, therefore, provide a sensitive measure of conformational differences among various forms of a protein or peptide. During the reduction of the native peptide with millimolar concentrations of DTT, only the native and fully reduced peptides were detectable at significant levels. It appears that once one disulfide of the native peptide is reduced under these conditions, the remaining two are cleaved at much higher rates so that there is no significant accumulation of intermediates with one or two disulfide bonds.

In Figure 7, the fraction of native peptide (filled symbols) remaining is plotted as a function of time. The data were well fit by a single exponential, consistent with the large molar excess of DTT present. Similar plots obtained for different reductant concentrations yielded pseudo-first-order rate constants that were proportional to the concentration of DTT. From these data, the second-order rate constant for the rate-determining step in the reduction was estimated to be 3 s^{-1} M^{-1}. This rate is approximately 5 times slower than that of the freely accessible disulfide in oxidized glutathione (Creighton, 1975; Szajewski & Whitesides, 1980;

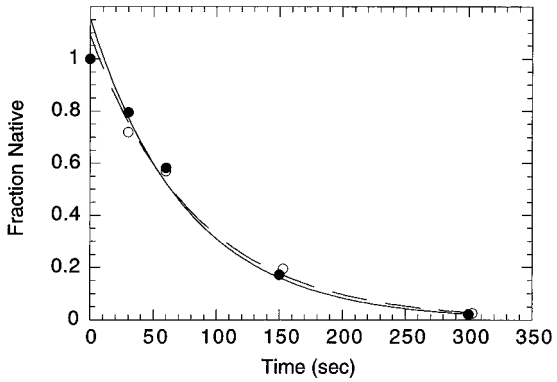

FIGURE 7: Kinetics of reductive unfolding of native and refolded ω-MVIIA in the presence of 5 mM dithiothreitol. Native (●) or refolded ω-MVIIA (○) were incubated in the presence of 5 mM DTT at 25 °C, pH 8.7. At the indicated times, samples of the reaction mixtures were quenched, and the disulfide-bonded molecules were fractionated by reversed-phase HPLC. The fraction of material with the HPLC retention time of the native peptide was determined from the peak areas. The curves represent least-squares fits of the data to an exponential decay function with apparent first-order rate constants of 0.013 and 0.012 s^{-1} for the native and refolded forms, respectively, corresponding to second-order rate constants of 2.6 and 2.4 s^{-1} M^{-1}.

Rothwarf & Scheraga, 1992), suggesting that even the most reactive disulfide of native ω-MVIIA is not fully accessible to DTT, consistent with the accessible surface area calculations described under Discussion.

The reduction kinetics of ω-MVIIA that had been reduced, refolded, and HPLC-purified was analyzed in the same way. As for the native peptide, there was no detectable accumulation of intermediates during reductive unfolding. In addition, the rates of reduction were indistinguishable for the native and refolded forms, as shown by the open and filled symbols in Figure 7. As for the native peptide, the reduction of the refolded ω-MVIIA was well described by a single exponential, as expected if the sample were homogeneous.

The kinetics of reductive unfolding of native ω-MVIIA were also examined using GSH as the reductant, under the same conditions used for the folding experiments. Reduction kinetics with this reagent are typically more complex than those observed with DTT, because reduction of the mixed-disulfide intermediate is usually much slower, allowing other reactions, including re-formation of the original disulfide or intramolecular rearrangements, to compete effectively (Creighton & Goldenberg, 1984). In contrast with the results obtained with DTT, numerous intermediates in the reduction reaction with GSH were detectable. Most strikingly, the nonnative three-disulfide forms identified in the refolding reactions were also seen in the early stages of reductive unfolding. Both the rate at which the native peptide disappeared and the transient appearance of the nonnative forms were accounted for by the scheme and rate constants shown in eq 2, as shown in Figure 8. The consistency between the observed and predicted reduction kinetics provides further evidence for the validity of the proposed model.

Disulfide-Coupled Folding of Other ω-Toxins. The ω-toxins that have been analyzed by NMR appear to have similar native conformations, although they display very little sequence similarity other than the disulfide-bonded Cys residues and the prevalence of polar residues. In order to determine whether the refolding efficiency observed for

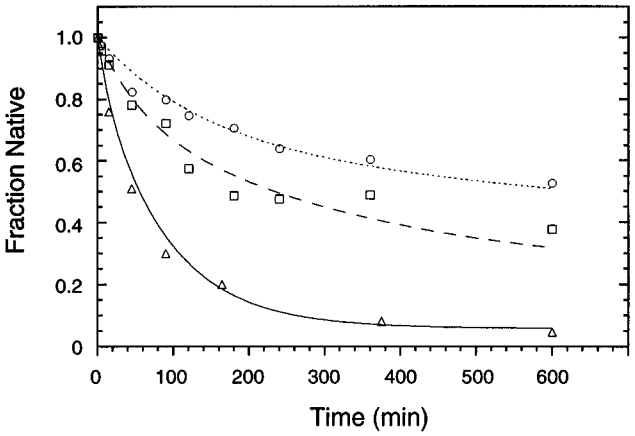

FIGURE 8: Kinetics of reductive unfolding of native ω-MVIIA in the presence of reduced glutathione. The native peptide was incubated in the in the presence of 0.5 mM (○), 1 mM (□), or 3 mM (△) GSH. At the indicated times, samples were quenched and the fraction of remaining native peptide was determined by HPLC. The curves shown represent the relative concentration of native peptide predicted by numerical simulations based on the scheme and rate constants shown in eq 2.

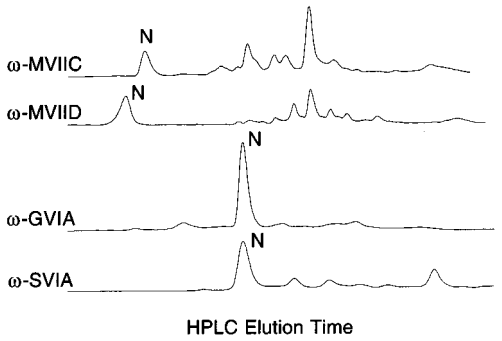

FIGURE 9: Disulfide-coupled folding of ω-conotoxins MVIIC, MVIID, GVIA, and SVIA. The native peptides were fully reduced and then refolded for 90 min in the presence of 1 mM GSSG and 2 mM GSH at 25 °C, pH 7.3, as described in the legend to Figure 2. The reactions were quenched by addition of 0.05 volume of concentrated H_3PO_4 and fractionated by reversed-phase HPLC. The peaks with the elution times of the native forms of each peptide are indicated.

ω-MVIIA is typical of other members of this family, refolding reactions for four other ω-toxins were examined under the conditions found to be optimal for ω-MVIIA. Figure 9 illustrates reversed-phase HPLC profiles obtained after folding of each of the toxins for 90 min in the presence of 1 mM GSSG and 2 mM GSH. For each profile, the elution time of the native form is indicated.

Two of the toxins examined, ω-GVIA and ω-SVIA, were found to refold with efficiencies similar to that observed for ω-MVIIA. These two toxins are found in the venoms of *Conus geographus* and *Conus striatus*, respectively, and have biological activities similar, though not identical, to that of ω-MVIIA. The sequences of ω-MVIIA, ω-GVIA, and ω-SVIA are all quite different from one another, however. Rather surprisingly, the two peptides most similar to ω-MVIIA were found to fold with considerably lower efficiencies, 16% and 28% for ω-MVIIC and ω-MVIID, respectively. The folding yields for these peptides were not increased when more oxidizing glutathione concentrations were used.

These results indicate that the folding efficiency depends upon the sequence of the ω-toxins, as well as the folding

conditions, but it is difficult at this time to conclude what features of the sequences are most important.

DISCUSSION

Work in other laboratories has previously demonstrated that several of the *Conus* toxins can correctly form their disulfides in vitro, with the yields varying greatly among the different peptides and with the conditions used (Zhang & Snyder, 1991; Pennington et al., 1990; Kim et al., 1995; Chung et al., 1995; Nadasdi et al., 1995). The work presented here extends some of these observations by systematically exploring some of the factors likely to influence folding rates and efficiency, using conditions that resemble those expected to be relevant in vivo, i.e., neutral pH and millimolar concentrations of oxidized and reduced glutathione. Using HPLC to monitor refolding, we have found that some of the ω-toxins are able to fold with efficiencies much greater than expected for random disulfide formation but that this efficiency is quite sensitive to the thiol−disulfide redox potential, the presence of a chaotropic denaturant, and the amino acid sequence. In the case of the peptide studied most extensively here, ω-MVIIA, the refolded molecules were shown to have the same biological activity and rate of reductive unfolding as the starting material, confirming that the HPLC peak associated with the native peptide does, in fact, contain predominantly molecules that have correctly refolded.

The overall folding rates for ω-MVIIA in the presence of various concentrations of GSSG and GSH could be accounted for by a relatively simple kinetic scheme and a single set of rate constants (eq 2). This model indicates that there is a kinetic partitioning between the native and nonnative three-disulfide forms, with a 15-fold greater rate for forming the nonnative species than the native peptide. The nonnative forms are also reduced much more rapidly, however, so that the final distribution favors the native form over any one of the nonnative species. The low relative rate of forming the native species may be due to a simple statistical factor, with the precursors to the nonnative three-disulfide forms representing a much larger fraction of the two-disulfide population than do the precursors to the native form. In addition, steric constraints associated with forming the buried disulfides, as is seen in some steps in the BPTI folding pathway, may inhibit formation of the native disulfides.

Although the simple model represented in eq 2 can account for the results observed here, it should not be taken as a detailed description of the folding mechanism. It is quite possible that there are significant kinetic barriers separating some of the intermediates grouped together as I, II, and II^{S-SG}. Also, the rate constants for the formation and reduction of I, II, and II^{S-SG} are not well defined by the present experiments, because no attempt has been made to quantify the levels of these populations individually. More detailed analyses of the folding ω-MVIIA and related molecules are currently in progress.

Comparing the folding rates and the final yields of native peptide observed in the presence of varying concentrations of GSSG and GSH (Figures 2 and 3) indicates that there are optimum conditions, where [GSSG] $\sim$ 1 mM and [GSH] $\sim$ 2 mM, for rapid and efficient folding. In the absence of added GSH, formation of the native form is extremely slow because other forms are generated preferentially and their conversion to the native form is limited by the small amount of GSH generated by the disulfide formation reactions. Under more reducing conditions, species with longer retention times, and probably containing one or two intramolecular disulfide bonds, become more significant. The GSH and GSSG concentrations for which the folding rates and yields were highest correspond quite well with those measured in the eukaryotic secretory pathway by Hwang et al. (1992), suggesting that the processes we are studying in vitro are compatible with in vivo conditions.

The final distributions generated in the presence of both GSSG and GSH appeared to represent an equilibrium population, since incubating the native protein under the same conditions generated a nearly indistinguishable HPLC profile (Figure 4). This observation suggests that the folding efficiencies of the ω-toxins is limited by the thermodynamic stability of the native protein, relative to those of other possible forms, rather than by large kinetic barriers, such as seen in the disulfide-coupled folding of BPTI (Creighton & Goldenberg, 1984; Weissman & Kim, 1991; Zhang & Goldenberg, 1993). The equilibrium distribution also enables us to estimate the overall equilibrium constant for the disulfide-coupled reaction:

$$R + 3GS\text{-}SG \rightleftharpoons N + 6GSH \qquad (4)$$

From the relative concentrations of the native and fully reduced forms measured in the presence of 1 mM GSSG and 20 mM GSH, the equilibrium constant for this reaction was estimated to be 0.04 M^3. For comparison, the corresponding equilibrium constants for forming single disulfides in unfolded polypeptides are typically in the range of 0.1−0.001 M, depending on the number of intervening residues (Snyder, 1987; Zhang & Snyder, 1989, 1991; Darby & Creighton, 1993). Thus, the overall equilibrium constant for forming three such independent disulfides would be about 10^{-6} M^3. Representing the other extreme, the overall equilibrium constant for the disulfide-coupled folding of BPTI, determined from kinetic folding and unfolding experiments, is approximately 10^4 M^3 [calculated from the data of Creighton and Goldenberg (1984)]. It thus appears that formation of the correctly disulfide-bonded form of ω-MVIIA is significantly more favorable than random Cys pairing in an unfolded polypeptide but that the disulfides are favored much less than in a more typically-sized globular domain, by approximately 7 kcal/mol.

As shown in Figure 5, the yield of correctly folded ω-MVIIA was reduced to about 10% in the presence of 8 M urea. This result suggests that noncovalent interactions, as opposed to steric effects arising from the number and types of residues lying between the Cys residues, play a major role in directing the correct formation of disulfides, as has been shown to be the case for other disulfide-bonded proteins. Although the mechanisms by which denaturants such as urea act are not fully understood, it is generally thought that they weaken the hydrophobic effect, thereby lessening the tendency for nonpolar groups to be buried in the folded conformation (Tanford, 1968; Schellman, 1978). The observed effects of urea thus suggest that the hydrophobic effect may play an important role in directing correct folding and disulfide formation in the ω-conotoxins.

In order to assess further the possible contribution of the hydrophobic effect, we calculated the accessibility of indi-

vidual atoms in folded ω-MVIIA to solvent. Empirical correlations suggest that the contribution of the hydrophobic effect to the stability of a folded conformation can be estimated, at least qualitatively, from the difference between the nonpolar surface area accessible in an extended conformation and that accessible in the folded structure, i.e., the amount of nonpolar surface area buried in the folded structure (Chothia, 1974, 1975; Richards, 1977; Eisenberg & McLachlan, 1986; Baldwin, 1986; Spolar et al., 1989, 1992). Accessibility calculations were carried out on each of 13 energy-minimized structures calculated by Kohno et al. (1995) from NMR constraints, and the results obtained for each residue were averaged. The average total accessible surface area for the 13 structures is 2170 (±70) Å^2, while that calculated for the individual residues in extended conformations is 4100 Å^2. Miller et al. (1987) have shown that monomeric globular proteins with molecular weights ranging from 4000 to 35 000 display a simple power-law relationship between molecular weight and total accessible surface area. This relationship predicts an accessible surface area of 1985 Å^2 for ω-MVIIA (with a molecular weight of 2639), very similar to that observed and consistent with the globular structure of the folded peptide.

For the 46 monomeric proteins examined by Miller et al. (1987), 47% of the solvent-accessible surface area is, on average, nonpolar, while 58% of the buried surface area is nonpolar. If the disulfide-bonded Cys sulfur atoms of ω-MVIIA are classified as polar, as in the analysis of Miller et al., then only 42% of the buried surface area is nonpolar. However, hydrophobicity scales based on measurements of transfer between water and nonpolar liquids generally indicate that transfer of a Cys side chain, in either the thiol or disulfide form, to a nonpolar environment is favorable, though perhaps less so than for a hydrocarbon of equivalent surface area (Fauchère & Pliska, 1983; Eisenberg & McLachlan, 1986; Abraham & Leo, 1987; Roseman, 1988; Saunders et al., 1993). If the Cys sulfur atoms of ω-MVIIA are classified as nonpolar, then 60% of the buried surface area is nonpolar, very similar to the values observed for larger protein domains, to which sulfur atoms make only a small contribution.

The large contribution of the Cys residues to the core of this peptide is illustrated further in Figure 10, where the buried nonpolar surface areas of the individual residues are plotted. For the Cys residues, the contributions of the sulfur atoms are indicated by the open portions of the bars. Five of the six Cys residues make the largest individual contributions to the nonpolar core, with the sulfur atoms representing the majority of the buried nonpolar surface area of each residue.

These calculations thus indicate that the distribution of polar and nonpolar atoms within the folded structure of ω-MVIIA is quite similar to that seen for larger proteins, except that the hydrophobic core is formed predominantly by the disulfide-bonded Cys residues. During folding of the reduced peptide, the correct pattern of disulfides may be favored simply because other possible patterns do not bury the Cys side chains so efficiently. In the presence of 8 M urea, the penalty for leaving these side chains exposed is probably reduced, thereby leading to a much more random distribution of disulfide-bonded forms.

In addition to the Cys residues, however, other features of the sequence can significantly affect the ability of the

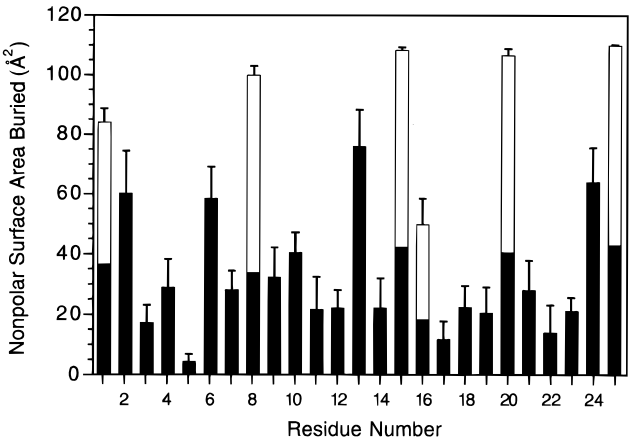

FIGURE 10: Nonpolar surface area buried in the folded conformation of ω-MVIIA. Buried surface area was calculated as the difference between the accessible surface area for a residue in an extended polypeptide and that for the residue in the folded conformation. Accessible surface areas were calculated for each of 13 NMR structures determined by Kohno et al. (1995), and the results for each residue were averaged. The error bars represent standard deviations of the results obtained for the 13 structures. All carbon and sulfur atoms were classified as nonpolar. The contributions of the sulfur atoms are represented by the open portions of the bars.

ω-conotoxins to fold, as indicated by the range of folding efficiencies observed for other members of the family (Figure 8). It is not clear, however, what features of the sequences are important for determining folding efficiency. Along with ω-MVIIA, the two peptides with the highest refolding yields were ω-GVIA and ω-SVIA. These two peptides share little similarity with one another or with ω-MVIIA. In contrast, ω-MVIIC and ω-MVIID have sequences very similar to that of ω-MVIIA but refold with much lower efficiencies. In their description of the solution structure of ω-MVIIC, Farr-Jones et al. (1995) note that all six of the disulfide-bonded sulfur atoms of this molecule are buried. Thus, the lower folding efficiency observed for ω-MVIIC does not appear to arise from less complete burial of the disulfides. To determine which non-Cys residues influence folding, it will probably be necessary to compare variants with fewer sequence differences than was possible in this study.

In summary, the results presented here indicate that some of the ω-conotoxins are able to fold and form the correct disulfides with surprisingly high efficiency and suggest that a major factor in the folding of these molecules may be burial of the disulfide-bonded Cys residues. Even for those molecules that fold most efficiently, however, the stability of the native structure, relative to other disulfide-bonded forms, is only marginal. These results suggest that other factors, such as precursor sequences or cellular proteins, may play important roles in facilitating folding in vivo. These possibilities are considered in the accompanying paper.

ACKNOWLEDGMENTS

We are particularly grateful to Professor B. M. Olivera for stimulating our interest in the folding of conotoxins and for making available to us several of the peptides used here, as well as materials and facilities for the synaptosome binding assay. Dr. T. Kohno kindly shared with us the coordinates of ω-MVIIA derived from NMR studies. The ω-MVIIA samples used were generous gifts of Drs. George Miljanich (Neurex Corp.) and Michael Gerlander (Bachem Inc., Torrance, CA). We also thank Lita Imperial for invaluable

assistance with the binding assays and Robert Schackmann for synthesis of some of the peptides at the protein/DNA core facility of the Utah Regional Cancer Center (supported by National Cancer Institute Grant 5 P30 CA42014).

REFERENCES

Abraham, D. J., & Leo, A. J. (1987) *Proteins: Struct. Funct. Genet. 2*, 130−152.

Baldwin, R. L. (1986) *Proc. Natl. Acad. Sci. U.S.A. 83*, 8069−8072.

Basus, V. J., Nadasdi, L., Ramachandran, J., & Miljanich, G. P. (1995) *FEBS Lett. 370*, 163−169.

Chothia, C. (1974) *Nature 248*, 338−339.

Chothia, C. (1975) *Nature 254*, 304−308.

Chung, D., Gaur, S., Bell, J. R., Ramachandran, J., & Nadasdi, L. (1995) *Int. J. Pept. Protein Res. 46*, 320−325.

Colledge, C. J., Hunsperger, J. P., Imperial, J. S., & Hillyard, D. R. (1992) *Toxicon 30*, 1111−1116.

Creighton, T. E. (1975) *J. Mol. Biol. 96*, 767−776.

Creighton, T. E. (1990) *Biochem. J. 270*, 1−16.

Creighton, T. E. (1992) in *Protein Folding* (Creighton, T. E., Ed.) pp 301−351, W. H. Freeman, New York.

Creighton, T. E., & Goldenberg, D. P. (1984) *J. Mol. Biol. 179*, 497−526.

Cruz, L. J., & Olivera, B. M. (1986) *J. Biol. Chem. 261*, 6230−6233.

Darby, N. J., & Creighton, T. E. (1993) *J. Mol. Biol. 232*, 873−896.

Davis, J. H., Bradley, E. K., Miljanich, G. P., Nadasdi, L., Ramachandran, J., & Basus, V. J. (1993) *Biochemistry 32*, 7396−7405.

Eisenberg, D., & McLachlan, A. (1986) *Nature 319*, 199−203.

Farr-Jones, S., Miljanich, G. P., Nadasdi, L., Ramachandran, J., & Basus, V. J. (1995) *J. Mol. Biol. 248*, 106−124.

Fauchère, J. L., & Pliska, V. (1983) *Eur. J. Chem. Chim. Ther. 18*, 369−375.

Frieden, C. (1993) *Trends Biochem. Sci. 18*, 58−60.

Glazer, A. N. (1976) in *The Proteins* (Neurath, H., & Hill, R. L., Eds.) Vol. II, pp 1−103, Academic Press, New York.

Goldenberg, D. P. (1992) *Trends Biochem. Sci. 17*, 257−261.

Goldenberg, D. P., Bekeart, L. S., Laheru, D. A., & Zhou, J. D. (1993) *Biochemistry 32*, 2835−2844.

Gray, W. R., Cruz, L. J., & Olivera, B. M. (1988) *Annu. Rev. Biochem. 57*, 665−700.

Hillyard, D. R., Monje, V. D., Mintz, I. M., Bean, B. P., Nadasdi, L., Ramachandran, J., Miljanich, G., Azimi-Zoonooz, A., McIntosh, J. M., Cruz, L. J., Imperial, J. S., & Olivera, B. M. (1992) *Neuron 9*, 69−77.

Hwang, C., Sinskey, A. J., & Lodish, H. F. (1992) *Science 257*, 1496−1502.

Kim, J. I., Takahashi, M., Ogura, A., Kohno, T., Kudo, Y., & Sato, K. (1994) *J. Biol. Chem. 269*, 23876−23878.

Kim, J. I., Takahashi, M., Ohtake, A., Wakamiya, A., & Sato, K. (1995) *Biochem. Biophys. Res. Commun. 206*, 449−454.

Kobayashi, Y., Ohkubo, T., Kyogoku, Y., Nishiuchi, Y., Sakakibara, S., Braun, W., & Go, N. (1989) *Biochemistry 28*, 4853−4860.

Kohno, T., Kim, J. I., Kobayashi, K., Kodera, Y., Maeda, T., & Sato, K. (1995) *Biochemistry 34*, 10256−10265.

Konishi, Y., Ooi, T., & Scheraga, H. A. (1982) *Biochemistry 21*, 4734−4740.

Lee, B., & Richards, F. M. (1971) *J. Mol. Biol. 55*, 379−400.

Li, Y. J., Rothwarf, D. M., & Scheraga, H. A. (1995) *Nature Struct. Biol. 2*, 489−494.

Lyles, M. M., & Gilbert, H. F. (1991) *Biochemistry 30*, 613−619.

Miller, S., Janin, J., Lesk, A. M., & Chothia, C. (1987) *J. Mol. Biol. 196*, 641−656.

Monje, V. D., Haack, J. A., Naisbitt, S. R., Miljanich, G., Ramachandran, J., Nasdasdi, L., Olivera, B. M., Hillyard, D. R., & Gray, W. R. (1993) *Neuropharmacology 32*, 1141−1149.

Nadasdi, L., Yamashiro, D., Chung, D., Tarczy-Hornoch, K., Adriaenssens, P., & Ramachandran, J. (1995) *Biochemistry 34*, 8076−8081.

Olivera, B. M., McIntosh, J. M., Cruz, L. J., Luque, F. A., & Gray, W. R. (1984) *Biochemistry 23*, 5087−5090.

Olivera, B. M., Cruz, L. J., de Santos, V., LeCheminant, G. W., Griffin, D., Zeikus, R., McIntosh, J. M., Galyean, R., Varga, J., Gray, W. R., & Rivier, J. (1987) *Biochemistry 26*, 2086−2090.

Olivera, B. M., Rivier, J., Clark, C., Ramilo, C. A., Corpuz, G. P., Abogadie, F. C., Mena, E. E., Woodward, S. R., Hillyard, D. R., & Cruz, L. J. (1990) *Science 249*, 257−263.

Olivera, B. M., Rivier, J., Scott, J. K., Hillyard, D. R., & Cruz, L. J. (1991) *J. Biol. Chem. 266*, 22067−22070.

Olivera, B. M., Miljanich, G. P., Ramachandran, J., & Adams, M. E. (1994) *Annu. Rev. Biochem. 63*, 823−867.

Pace, C. N., & Creighton, T. E. (1986) *J. Mol. Biol. 188*, 477−486.

Pallaghy, P. K., Duggan, B. M., Pennington, M. W., & Norton, R. S. (1993) *J. Mol. Biol. 234*, 405−420.

Pallaghy, P. K., Nielsen, K. J., Craik, D. J., & Norton, R. S. (1994) *Protein Sci. 3*, 1833−1839.

Pardi, A., Galdes, A., Florance, J., & Maniconte, D. (1989) *Biochemistry 28*, 5494−5501.

Pennington, M. W., Festin, S. M., & Maccecchini, M. L. (1991) in *Peptides 1990* (Giralt, E., & Andreu, D., Eds.) ESCOM Science, Leiden, The Netherlands.

Ponder, J. W., & Richards, F. M. (1987) *J. Mol. Biol. 193*, 775−791.

Radzicka, A., & Wolfenden, R. (1988) *Biochemistry 27*, 1664−1670.

Ramilo, C. A., Zafaralla, G. C., Nadasdi, L., Hammerland, L. G., Yoshikami, D., Gray, W. R., Kristipati, R., Ramachandran, J., Miljanich, G., Olivera, B. M., & Cruz, L. J. (1992) *Biochemistry 31*, 9919−9926.

Richards, F. M. (1977) *Annu. Rev. Biophys. Bioeng. 6*, 151−176.

Roseman, M. A. (1988) *J. Mol. Biol. 200*, 513−522.

Rothwarf, D. M., & Scheraga, H. A. (1992) *Proc. Natl. Acad. Sci. U.S.A. 89*, 7944−7948.

Rothwarf, D. M., & Scheraga, H. A. (1993) *Biochemistry 32*, 2671−2679.

Saunders, A. J., Young, G. B., & Pielak, G. J. (1993) *Protein Sci. 2*, 1183−1184.

Saxena, V. P., & Wetlaufer, D. (1970) *Biochemistry 9*, 5015−5023.

Schellman, J. A. (1978) *Biopolymers 17*, 1305−1322.

Singh, R., & Whitesides, G. M. (1990) *J. Am. Chem. Soc. 112*, 6304−6309.

Sevilla, P., Bruix, M., Santoro, J., Gago, F., Garcia, A. G., & Rico, M. (1993) *Biochem. Biophys. Res. Commun. 192*, 1238−1244.

Skalicky, J. J., Metzler, W. J., Ciesla, D. J., Galdes, A., & Pardi, A. (1993) *Protein Sci. 2*, 1591−1603.

Snyder, G. H. (1987) *Biochemistry 26*, 688−694.

Spolar, R. S., Ha, J.-H., & Record, M. T. (1989) *Proc. Natl. Acad. Sci. U.S.A. 86*, 8382−8385.

Spolar, R. S., Livingstone, J. R., & Record, T. M. (1992) *Biochemistry 31*, 3947−3955.

Szajewski, R. P., & Whitesides, G. M. (1980) *J. Am. Chem. Soc. 102*, 2011−2026.

Tanford, C. (1968) *Adv. Protein Chem. 23*, 121−282.

Wearne, S. J., & Creighton, T. E. (1988) *Proteins: Struct., Funct., Genet. 4*, 251−261.

Weissman, J. S., & Kim, P. S. (1991) *Science 253*, 1386−1393.

Woodward, S. R., Cruz, L. J., Olivera, B. M., & Hillyard, D. R. (1990) *EMBO J. 9*, 1015−1020.

Zhang, J. X., & Goldenberg, D. P. (1993) *Biochemistry 32*, 14075−14081.

Zhang, R., & Snyder, G. H. (1989) *J. Biol. Chem. 264*, 18472−18479.

Zhang, R., & Snyder, G. (1991) *Biochemistry 30*, 11343−11349.

BI961574C